Applied Catalysis A: General 375 (2010) 17–25

Contents lists available at ScienceDirect

Applied Catalysis A: General

journal homepage: www.elsevier.com/locate/apcata

Kinetics and mechanism of partial oxidation of ethane to ethylene and acetic acid over MoV type catalysts

Faizur Rahman [a,*], Kevin F. Loughlin [b,d], Muhammad A. Al-Saleh [b], Mian R. Saeed [a], Nasir M. Tukur [b], Mohammad M. Hossain [b], Khalid Karim [c], Agaddin Mamedov [c]

[a] Center of Research Excellence in Petroleum Refining & Petrochemicals, Research Institute, King Fahd University of Petroleum & Minerals, Dhahran, Saudi Arabia
[b] Department of Chemical Engineering, King Fahd University of Petroleum & Minerals, Dhahran, Saudi Arabia
[c] SABIC Research and Technology, Riyadh, Saudi Arabia
[d] American University of Sharjah, United Arab Emirates

ARTICLE INFO

Article history:
Received 4 March 2009
Received in revised form 17 November 2009
Accepted 18 November 2009
Available online 24 November 2009

Keywords:
Ethane partial oxidation
Ethylene
Acetic acid
Reaction network
Kinetic model
Eley-Rideal-Redox model
MoV type catalyst
Reaction mechanism

ABSTRACT

A kinetics study for the partial oxidation of ethane to ethylene and acetic acid is performed over MoV type catalysts. It is established that ethylene is the primary product and acetic acid and carbon oxides are secondary products. Formation of acetic acid product increases significantly with the co-feeding of water into the reactor. The elementary steps of the reaction network are formulated using a two-site Eley-Rideal-Redox (ERR) model, which includes the participation of water in the reaction scheme through surface OH^- groups. The derived ERR model predicts the experimental data satisfactorily.

1. Introduction

In recent years the production of ethylene and acetic acid from the partial oxidation of ethane has developed as an alternative route to provide feedstock to the downstream petrochemical industry. Mixed oxides catalysts containing molybdenum and vanadium are the preferred catalyst for this investigation [1–15].

The key fact concerning these mixed oxide catalyst [16] is their multiphase nature which strongly influences the mechanism and the kinetics of the partial oxidation of ethane. Desponds et al. [3] indicated that three oxide phases were necessary to have active and selective catalysts.

Linke et al. [9,10] used a $MoV_{0.25}Nb_{0.12}Pd_{0.0005}O_x$ based catalyst in their study of this reaction. They suggested the existence of two different catalytic centers, one for the oxidative dehydrogenation of ethane, and one for the heterogeneous Wacker oxidation of ethylene to acetic acid. The latter site arises from the formation of highly dispersed Pd(II) sites into an Mo_5O_{14} phase promoting the Wacker hydroxylation reaction. Thornsteinson et al. [1] suggested various mixed oxide catalysts containing Mo and V together with transition metal oxides (Ti, Cr, Mn, Fe, Co, Ni, Nb, Ta or Ce) promoted partial oxidation reactions. The optimum composition was observed to be $Mo_{0.61}V_{0.31}Nb_{0.08}$ for reaction of ethane to ethylene. The presence of niobium stabilizes the catalyst structure against oxidation and reduction and permits a very strongly oxidized or reduced catalyst to be recycled more readily to its original value. Rouessel et al. [12] observed two phases, $MoV_{0.4}O_x$ and $MoV_{0.4}Nb_{0.12}O_x$, and found that niobium is responsible for both stabilization and nanosizing of MoO_3 and $(VNbMo)_5O_{14}$ crystals. Surface oxygen, OH groups, and oxygen vacancies are the most abundant reactive sites during ethane oxidative dehydrogenation (ODH) on active VO_x domains of vanadium oxide (VO_x/Al_2O_3 and VO_x/ZrO_2) catalysts [20]. Ruth et al. [5] showed that the $Mo_6V_9O_{40}$ phase in a multiphase catalyst led to the formation of acetic acid. Catalytic experiments on pure VPO phases and titania supported VPO_x and VO_x are discussed by Tessier et al. [23] for the selective oxidation of ethane to acetic acid. The reaction mechanism is

* Corresponding author at: Box 1634, Dhahran 31261, Saudi Arabia.
Tel.: +96 6502662711; fax: +96 638694509.
E-mail addresses: rahman.faiz@gmail.com, frahman@kfupm.edu.sa (F. Rahman).

0926-860X/$ – see front matter © 2010 Published by Elsevier B.V.
doi:10.1016/j.apcata.2009.11.026

Nomenclature

A	Arrhenius pre-exponential factor typically (μmol/g/s)
A_1	defined as equal to $K_1 \times K_2$ in Table 4
A_2	defined as equal to $K_{10} \times K_{11}$ in Table 4
C_i	concentration of species i (μmol/cm^3)
CO_x	carbon oxides
E_i	activation energy (kJ/mol)
H_i	enthalpy of species i (J/μmol)
$-\Delta H$	heat of formation of products (J/μmol, transport limitation)
$(-\Delta H)_{Ri}$	enthalpy of reaction of species i (J/μmol)
K_i	adsorption equilibrium constant (cm^3/μmol)
K_e	equilibrium constant (dimensionless)
k_i	specific reaction rate constant (reaction order units)
LO	lattice oxygen
n	overall reaction order
P	reaction pressure (bar)
r_i	rate of reaction of species i per unit volume (μmol/g/s)
R_i	overall rate of reaction of species i per unit volume (μmol/g/s)
X	active site
XO	active oxygen center
XOH	hydroxylated X site
T	reaction temperature (K)
Z	active site
ZOH	hydroxylated Z site

Subscripts

i	species

Greek symbols

θ_i	fraction of the surface coverage by species i
ν	Stoichiometric coefficient

strongly dependent on the multiphase nature of the catalyst, which is supported by the two-site mechanisms [8,10]. The basic mechanism is reduction of the catalyst by the adsorbed hydrocarbon, reoxidation by oxygen [1,2,8,10,13,22] and surface hydroxylation by water [1,10,13]. The role of lattice oxygen in the reactions due to an active phase based on molybdenum and vanadium oxides has been reported by several authors [2,4,10]. Panov et al. [24] pointed out that, strongly bonded lattice oxygen having nucleophilic nature is responsible for selective oxidation whereas weakly bonded reactive oxygen having electrophilic nature contributes to complete oxidation. Sehgal [25] performed oxidative dehydrogenation of ethane over transition metal oxides and proposed that ethylene is formed by a redox mechanism of Mars and van Krevelen with the involvement of lattice oxygen species (O^{2-}) and surface oxygen species (O^-). The deep oxidation of both ethane and ethylene to CO and CO_2 is attributed to gas phase oxygen species. Capek et al. [26] investigated the performance of V-HMS, V-MCM41 and V-SBA-15 catalysts with varying vanadium loadings for the oxidative dehydrogenation of ethane. They concluded that the most active catalysts contained 2–4.5% V finely dispersed over mesoporous support in the form of isolated monomeric and oligomeric vanadium species and exhibited comparable activity.

Linke et al. [9–11], Smejkal et al. [16] and Grabowski and Sloczynski [13] indicate that the presence of water increases the formation of acetic acid but Desponds et al. [3] report that the addition of water to the gas stream does not affect the product distribution. The presence of niobium [1,3,15] or potassium [13] or adsorbed water which promotes desorption of acetic acid [15] inhibits the formation of carbon oxides.

The kinetics of reaction on these multiphase catalysts is primarily redox and most kinetic models are based on this principle. The kinetic models employed are redox [10], Eley-Rideal [4,8,13], and Langmuir-Hinshelwood [1]. Most studies indicate that the reaction order for ethane is close to 1, whereas for oxygen it is close to zero [2,4,8]. Thornsteinson et al. [1] indicate that the reaction rates to acetic acid and carbon oxides are dependent on the ethylene concentration but are independent of the ethane concentration.

Linke et al. [10] developed a set of elementary equations based on the redox principle for their two-site catalyst. The model has some deficiencies particularly in the elementary steps of deep oxidation reactions. The rate equations for ethane oxidation show no participation of water. However, acetic acid formation from ethylene is promoted in the presence of the oxydehydrogenation reaction. The elementary reaction steps 3, 4, 5, 9, 10 and 11 in their paper omit oxygen in their reaction steps. Each of the reactions on the left contains O_2, yet none of the rate equations on the right side contain oxygen in their rate expression. The activation energies for the reactions number 6 and 8 are negative. The redox reactions are also not balanced in determining the fractions adsorbed.

In this paper, a comprehensive kinetics study is presented based on mechanistic principles. In the literature, the effect of water on the kinetics of ethane oxidation is not yet clearly described. Some authors explain the physical adsorption of water on the surface of the catalyst. Chemical participation of water in elementary steps with the formation of surface intermediate has not been described. This paper explains the kinetics investigation describing the chemical interaction of water to the reaction mechanism. Considering water as participating in the reaction, kinetics models are derived explaining the effect of water to the different pathway of ethane oxidation. An independent study[1] using deuterated water confirmed this effect resulting in its incorporation in the kinetic model. The kinetic model based on mechanistic principles is evaluated using experimental data.

2. Experimental

The kinetic experiments were conducted using Mo-V based catalysts in a fixed bed flow reactor under differential reaction conditions. The details of catalyst preparation used in this study are described in terms of compositions [14,21]. Systematic data were generated to investigate the kinetics of C_2H_6 oxidation with and without water in the feed.

The kinetic experiments were performed using 0.15 g of catalyst diluted with inert material in a fixed bed flow reactor (ID = 0.78 cm) under differential reaction conditions. The reactor was maintained at temperatures ranging between 513 and 553 K, pressures in the range of 150–200 psig and at different space velocities. All the data are within the acceptable range of mass balance ±5% and the conversion of ethane is limited to less than 10%. Transport limitations in the reactor, estimated using the procedure described in references [17,19] showed that data generated for the kinetic studies are free from internal and external heat and mass transfer effects. For the kinetic investigation, a matrix of experiments is performed solely in a differential reactor at three levels of

[1] Personal Communication, SABIC, 2005.

Table 1
Experimental conditions for kinetic parameter evaluation.

Parameter	Partial oxidation of ethane
Catalyst weight (g)	0.15
Temperature (K)	513, 533, 553
Pressure (bar)	14
Volumetric flow (cm^3/min)	30
Space velocity (min^{-1})	205
Feed composition	
Ethane (mol%)	30–60
Oxygen (mol%)	6–12
Steam (mol%)	0
Nitrogen (mol%)	Balance

temperature, ethane concentration and oxygen concentration as illustrated in Table 1.

The products of ethane oxidation are C_2H_4, CH_3COOH, and CO_2. The conversions are calculated from the outlet flow rate of unreacted C_2H_6 and the amount of C_2H_6 reacted to form products C_2H_4, CH_3COOH and CO_2 considering the stoichiometry of the individual reactions.

3. Results and discussions

3.1. Effect of reactant concentration on ethane oxidation

The rate of ethane consumption and the rate of formation of products ethylene and acetic acid increase almost linearly with increasing concentration of ethane as illustrated in Fig. 1. On the other hand, the effect of O_2 concentration on the rate of C_2H_6 oxidation and on the rate of formation of products (C_2H_4, CH_3COOH and CO_2) appears to be insensitive when oxygen to ethane ratio is around 0.2 as can be observed in Fig. 2. Kinetic data implies that the selective oxidation of ethane is approximately first order with respect to ethane and is consistent with a mechanism in which the breaking of a C–H bond is rate determining. The reaction was found to be almost independent of the oxygen concentration, indicating that at reaction conditions the surface of the catalyst is fully oxidized, which is consistent with other reported data [2,5,20].

3.2. Effect of temperature

The conversion of C_2H_6 and product selectivities as a function of temperature at constant space velocity, and its impact on the product selectivity is illustrated in Fig. 3. As the reaction temperature increases, the conversion of ethane increases while

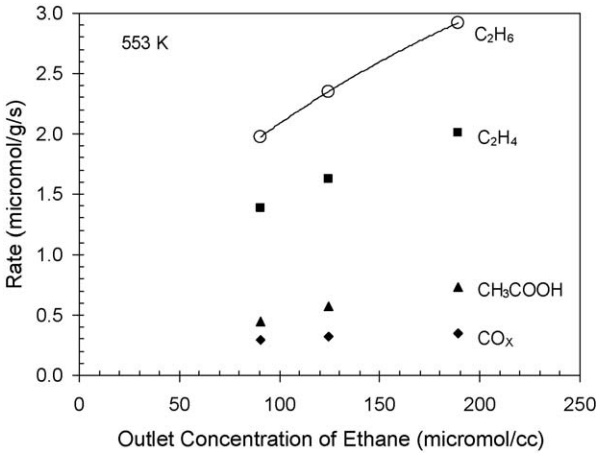

Fig. 1. Effect of variation in ethane concentration on reaction rates at 553 K (catalyst weight: 0.15 g, ethane to oxygen ratio: 4–9).

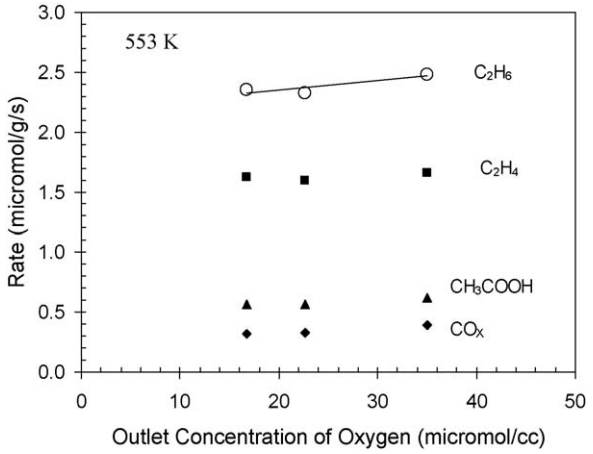

Fig. 2. Effect of variation in oxygen concentration on reaction rates at 553 K (catalyst weight: 0.15 g, ethane to oxygen ratio: 3–6).

the selectivity to ethylene decreases. The selectivity to CH_3COOH and CO_x increases with temperature at the expense of C_2H_4. This indicates C_2H_4 is a significant source of CH_3COOH and CO_x. The main products were found to be ethylene and acetic acid with selectivity of 50% and 30%, respectively, at 553 K.

3.3. Effect of space velocity

To elucidate the reaction network, experiments were performed at various space velocities. The selectivity of products for the partial oxidation of ethane without steam in the feed as a function of conversion of ethane is illustrated in Fig. 4. Ethylene appears as the primary product of reaction of the partial oxidation of ethane. The decrease in ethylene concentration with corresponding increase in CH_3COOH and CO_x indicates that these are the secondary products of consecutive oxidation of ethylene. Ethane does not appear to be the source of the products CH_3COOH, CO_2, and CO. The selectivity of products for the partial oxidation of ethylene as a function of conversion of ethylene is illustrated in Fig. 5. This figure clearly indicates that ethylene is the source of the products CH_3COOH, and CO_x and supports the results of Fig. 4.

A selectivity study separately performed in the reactor operating under integral mode (using catalyst = 7 g, ethane (mol%) = 5–25, oxygen (mol%) = 16–20, steam = 0, T (K) = 483–

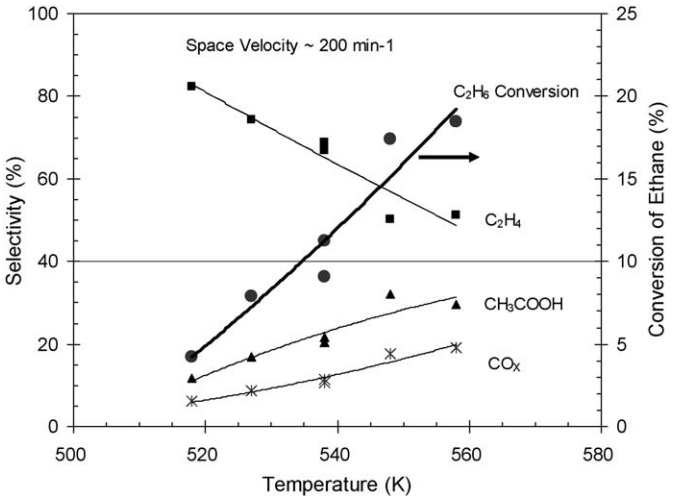

Fig. 3. Conversion of C_2H_6 and selectivity of products as a function of temperature at constant space velocity (catalyst weight: 0.2 g, C_2/O_2 = 0.8, P: 14 bar).

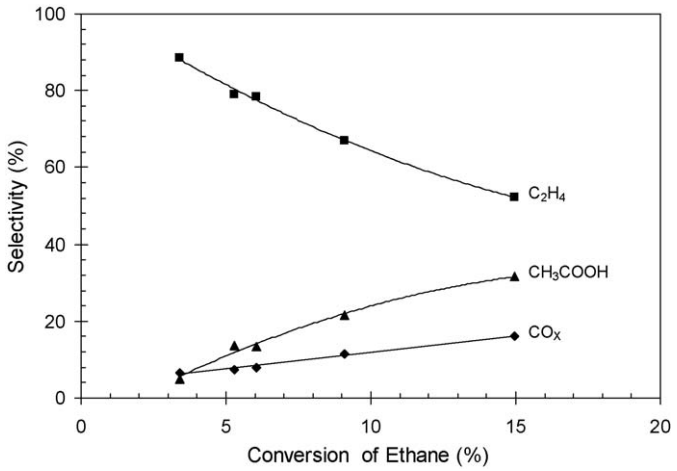

Fig. 4. Selectivity of products as a function of C_2H_6 conversion. Varying space velocity (T = 538 K, C_2H_6 = 14 mol%, O_2 = 17 mol%).

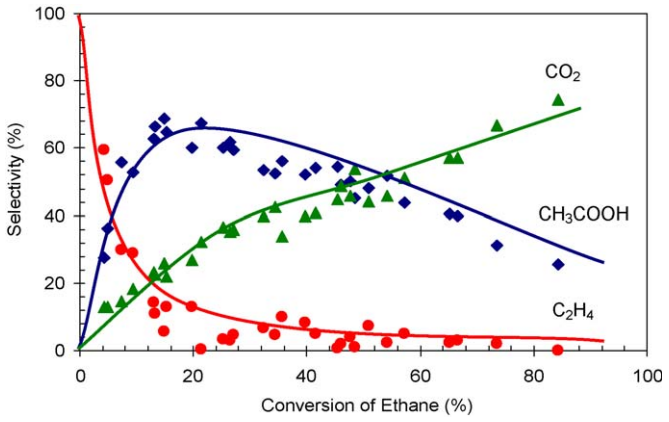

Fig. 6. Product selectivity versus ethane conversion in an integral reactor without steam in feed (solid lines represent trend lines; catalyst weight: 7 g, T: 483–553 K, P: 14 bar, C_2H_6: 5–25 mol%, O_2: 16–20 mol%, H_2O: 0).

563) presented in Fig. 6, confirms that as the conversion of ethane increases, ethylene converts to acetic acid forming acetic acid and carbon oxides. The acetic acid increases to a maximum and then decreases due to decomposition of acetic acid to carbon oxides.

This increase of acetic acid selectivity with ethylene conversion shows that acetic acid is produced from ethylene. Acetic acid selectivity increase is in the range of 0–20% ethylene conversion as may be observed in Fig. 5. The increase of acetic acid selectivity in Fig. 5 can be related to the influence of water formed in the reaction, i.e. the higher the degree of ethylene conversion, the higher the partial pressure of water. The co-feeding of water experiments also supports this explanation showing a significant increase of acetic acid selectivity with a decrease of ethylene selectivity. Therefore, Figs. 5 and 6 delineate all the direct and consecutive reactions. CO in the case of ethylene conversion forms in parallel reaction. That is why the selectivity extrapolation of CO to zero conversion is not zero as it becomes an intermediate due to its deep oxidation to CO_2.

Based on the above observation the possible reactions of the partial oxidation of C_2H_6 in the light of above discussion are:

$$C_2H_6 + 0.5O_2 \rightarrow C_2H_4 + H_2O \quad (1)$$

$$C_2H_6 + 1.5O_2 \rightarrow CH_3COOH + H_2O \quad (2)$$

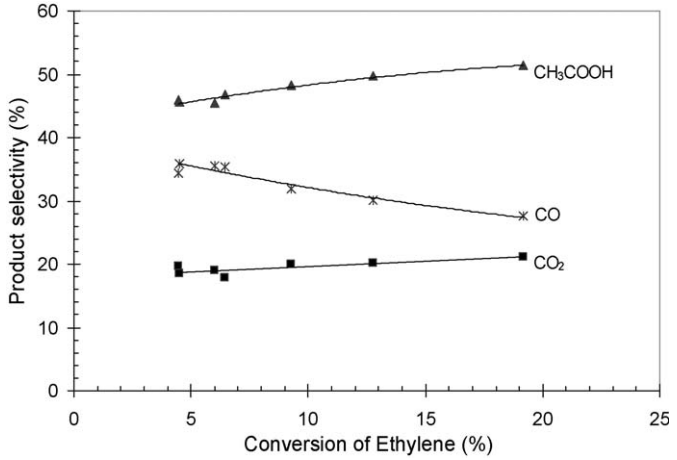

Fig. 5. Selectivity of products as a function of C_2H_4 conversion. Varying space velocity (T: 538 K, constant feed composition $C_2H_4 \sim 7$ mol%, $O_2 \sim 19.5$ mol%).

$$C_2H_6 + 2.5O_2 \rightarrow 2CO + 3H_2O \quad (3)$$

$$C_2H_6 + 3.5O_2 \rightarrow 2CO_2 + 3H_2O \quad (4)$$

$$C_2H_4 + O_2 \rightarrow CH_3COOH \quad (5)$$

$$C_2H_4 + 2O_2 \rightarrow 2CO + 2H_2O \quad (6)$$

$$C_2H_4 + 3O_2 \rightarrow 2CO_2 + 2H_2O \quad (7)$$

$$CH_3COOH + O_2 \rightarrow 2CO + 2H_2O \quad (8)$$

$$CH_3COOH + 2O_2 \rightarrow 2CO_2 + 2H_2O \quad (9)$$

$$CO + 0.5O_2 \rightarrow CO_2 \quad (10)$$

The reaction network scheme shown in Fig. 7 illustrated that ethane reacts only by route 1 to form ethylene is deduced from Fig. 4. Reaction (1) is the primary reaction. No parallel reactions of ethane occur implying reactions (2), (3) and (4) may be eliminated from network stoichiometric reaction schemes.

Ethylene reacts in parallel mode simultaneously forming the products CH_3COOH, CO_2, and CO as illustrated in Fig. 5 implying that reactions (5), (6) and (7) exist in the network. Two parallel reactions for the reaction of acetic acid to carbon monoxide and carbon dioxide occur (steps 8 and 9). Finally, reaction (10), a sequential reaction of carbon monoxide to carbon dioxide occurs

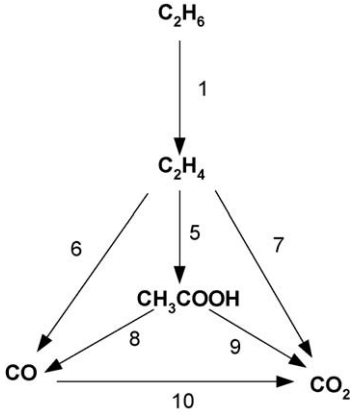

Fig. 7. Proposed reaction scheme for oxidation of C_2H_6 based on data without steam in feed.

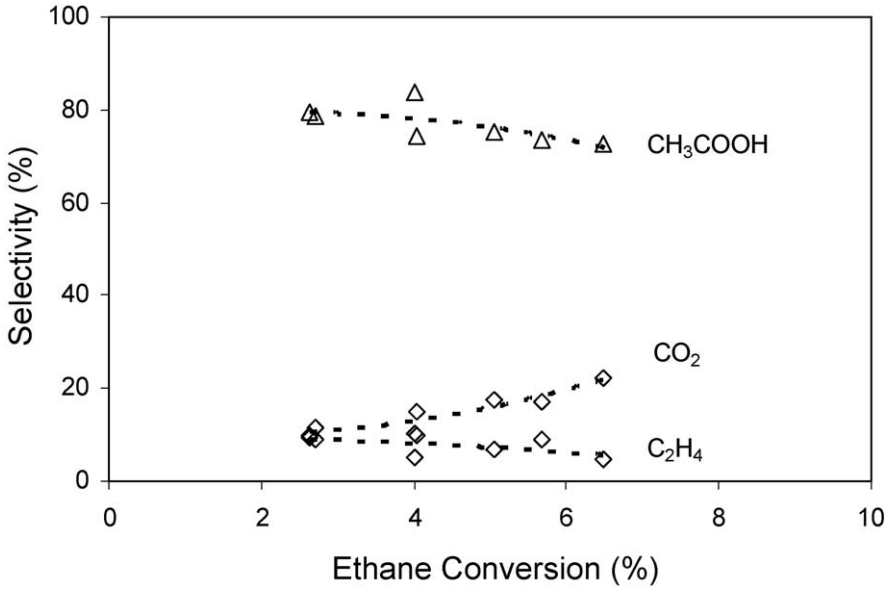

Fig. 8. Product selectivity versus conversion of C_2H_6 with steam in feed at varying space velocity (T = 553 K, P = 14 bar, C_2H_6 = 40 mol%, O_2 = 8 mol%, H_2O = 20 mol%, N_2 = 32 mol%).

based on an independent study carried out using carbon monoxide alone as a feed.

The study of the effect of co-feeding of water on the product distribution for partial oxidation of ethane showed a significant increase of acetic acid selectivity with a decrease of ethylene selectivity. The selectivity of products as a function of C_2H_6 conversion is illustrated in Fig. 8. The product distribution has completely reversed in terms of C_2H_4 and CH_3COOH as compared to data without co-feed of water (Fig. 4). The selectivity to CH_3COOH has increased significantly at the expense of C_2H_4. It is postulated that this increase in CH_3COOH selectivity with addition of water to the feed is due to oxy-hydoxylation reaction of C_2H_4 with water. Isotopic experiments using deuterated water (D_2O) in the feed confirmed that D_2O is participating in the reaction to form acetic acid.

Probably the increase of acetic acid selectivity with addition of water is connected with the participation of OH^- group generated from water in the elementary stage of the acetic acid formation. On the basis of these experiments it has been suggested that acetic acid formation proceeds through two routes: first nucleophilic oxygen centers participate in the elementary step in the insertion to ethylene molecule and in the second route OH^- groups lead to the formation of hydroxyl containing ethylene fragments, which in consecutive reactions form acetic acid.

Based on the selectivity versus ethane conversion data with steam in the feed and from the information revealed by isotopic experiments it is postulated that CH_3COOH is formed from ethylene via both an oxygen route and a hydroxyl route.

In view of above discussion, the reaction scheme proposed in Fig. 7 is modified to that in Fig. 9 for the reaction network.

3.4. Kinetic Model

Several reaction mechanisms such as Langmuir-Hinshelwood, Eley-Rideal, Redox, etc. were investigated to represent the experimental data. The description of experimental data using two types of active sites is based on the variation of catalyst composition and acidic or basic properties: increase of basic properties of the catalysts leads to increase of ethylene selectivity, for example the results on ethane dehydrogenation to ethylene on MoVMn containing catalyst [14]. Increase of acid properties leads to the increase of acetic acid selectivity. Basic idea of using two-site mechanism is that acid product forms on acid sites and desorbs faster from acid sites while the basic products (ethylene has much more basic property than acetic acid) forms on basic site and desorbs faster from basic site. Multicomponent catalyst studied in our work has multiphase catalytic structure suggesting two types of active sites, which is very common in oxidative catalysis with separation of reaction steps between the active sites. This idea also corresponds with the literature data that dehydrogenation proceeds with participation of basic property nucleophilic centers, while acid property products form with participation of electrophilic oxygen centers [14].

Eventually, a two-site kinetic model based on combined Eley-Rideal and Redox mechanisms was observed to render successful regression results with the experimental data. Consequently, the resulting model is named as an Eley-Rideal-Redox (ERR) model. The ERR kinetic model is a comprehensive model considering the

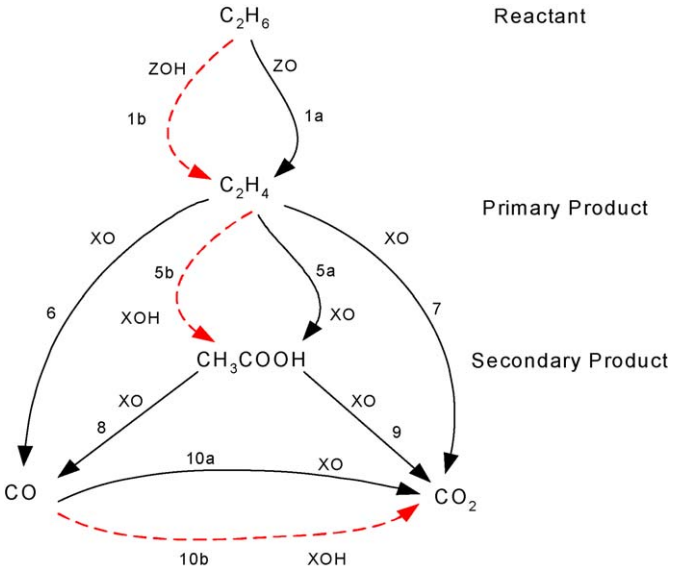

Fig. 9. Comprehensive proposed reaction scheme.

overall reaction scheme illustrated in Fig. 9. The following are the general principles on which the model is based:

I. Two sites, Z and X centers, are employed in the derivation of the reaction kinetics for the network system. This is consistent with the multiphase nature of the catalyst and literature work supporting this concept [6,8,10].
II. In the reaction from ethane to ethylene, two routes are shown, one via the oxide ZO type center and one via the hydroxyl ZOH type center. Also two routes are indicated in the transformation of ethylene to acetic acid, one via the oxide XO type center and one via the hydroxyl XOH type center. Similarly, two routes are indicated in the reaction of CO to CO_2, one via the oxide XO type center and one via the hydroxyl XOH type center.
III. In the presence of lattice oxygen centers, the introduction of water leads to the formation of hydroxyl species. Acidic nature of the Mo, V oxide phases of the mixed oxide catalyst may contribute to the realization of reaction with the formation of a surface OH^- center.

$$O^{2-} + HOH \Leftrightarrow 2OH^-$$

However at higher concentration of water, these centers are blocked due to physical adsorption.

$$Me^{n+} + H_2O + OH^- \Leftrightarrow Me^{n+}OH^-(H_2O)_{ads}$$

IV. On the X type site, ethylene reacts with either lattice oxygen or reacts with the hydroxyl group center by an Eley-Rideal mechanism. Again, a surfeit of water present on the site may result in the blocking of sites.

The shift in the behavior of catalyst in the formation of acetic acid without water and with addition of water in the feed posed difficulties during development of elementary steps. The increase in acetic acid formation due to the addition of water in the feed was solved by having two routes for the formation of CH_3COOH through the oxidation and hydroxylation of C_2H_4. The ERR Model describes the participation of water as well.

The existence of parallel mechanism of acetic acid formation with participation of oxide and OH groups is proved by isotopic experiments: Water added to the reaction feed was replaced by D_2O. During similar experiments as performed with H_2O, the acetic acid product was observed to be containing deuterium, proving the insertion of OD^- group in the acetic acid through surface oxygen centers in accordance with the suggested mechanism:

$$D_2O + O^{2-} \rightarrow 2OD^-$$

The elementary steps of the reaction are presented in Table 2 using the reaction scheme proposed in Fig. 9. The elementary steps are based on two independent sites labeled Z-site center and X-site center. Consider the Z-site first. Steps 1 and 2 are simply reversible adsorption of oxygen and dissociation with formation of surface oxygen species similar to that postulated by Linke et al. [10]. The oxygen species forms a lattice oxygen species LO. In step 3, water reacts with the ZO center to form surface hydroxyl species ZOH. When the ZO centers are fully used up or limited by the lack of ample oxygen, reversible physical adsorption of water can also occur on these sites, which block the surface.

On the Z-site ethane reacts from the gas phase with lattice oxygen sites to form a C_2H_5LOH, as shown in step 6, which is the rate determining step (RDS). The C_2H_5LOH species then rapidly decomposes in step 7 to produce ethylene. Similarly, it was postulated that ethylene also forms through a hydroxyl species in step 8 and 9. However, the formation of ethylene via steps 8 and 9 was later found insignificant or difficult to isolate through modeling results and is excluded from further discussions.

Table 2
Elementary steps based on reaction scheme in Fig. 9.

Step	Reaction
Reactions on Z type site	
1	$Z + O_2 \overset{1}{\longleftrightarrow} ZO_2$
2	$ZO_2 + Z \overset{2}{\longleftrightarrow} 2ZO$
3	$Z + ZO + H_2O \overset{3}{\longleftrightarrow} 2ZOH$
4	$ZOH + H_2O \overset{4}{\longleftrightarrow} ZOH(H_2O)$
5	$L + ZO \leftrightarrow Z + LO$
6	$C_2H_6 + LO \overset{6.RDS}{\longrightarrow} C_2H_5LOH$
7	$C_2H_5LOH \overset{fast}{\longrightarrow} C_2H_4 + H_2O + L$
8	$C_2H_6 + ZOH \overset{8.RDS}{\longrightarrow} C_2H_5Z + H_2O$
9	$C_2H_5Z + ZOH \overset{fast}{\longrightarrow} C_2H_4 + H_2O + 2Z$
Reactions on X type site	
10	$X + O_2 \overset{10}{\longleftrightarrow} XO_2$
11	$XO_2 + X \overset{11}{\longleftrightarrow} 2XO$
12	$H_2O + X + XO \overset{12}{\longleftrightarrow} 2XOH$
13	$XOH + H_2O \overset{13}{\longleftrightarrow} XOH(H_2O)$
14	$C_2H_4 + XO \overset{14}{\longleftrightarrow} C_2H_4XO$
15	$C_2H_4XO \overset{15.RDS}{\longrightarrow} CH_3CHOX$
16	$CH_3CHOX + XO \overset{fast}{\longrightarrow} CH_3COOH + 2X$
17	$C_2H_4XO + XOH \overset{17.RDS}{\longrightarrow} CH_3CHXOH + XO$
18a	$CH_3CHXOH + XO \rightarrow CH_3CXOH + XOH$
18b	$CH_3CXOH + XO \rightarrow CH_3COOHX + X$
18c	$CH_3COOHX \leftrightarrow CH_3COOH + X$
19	$C_2H_4XO + X \overset{19.RDS}{\longrightarrow} [\bullet]$
20	$[\bullet] + XO \overset{fast}{\longrightarrow} HCHOX + X$
21	$HCHOX + XO \overset{fast}{\longrightarrow} CO + H_2O + 2X$
22	$C_2H_4XO + XO \overset{22.RDS}{\longrightarrow} 2HCHOX$
23	$HCHOX + 2XO \overset{fast}{\longrightarrow} CO_2 + H_2O + 3X$
24	$CH_3COOH + XO \overset{24}{\longleftrightarrow} CH_3COOH \cdot XO$
25	$CH_3COOH.XO + 2X \overset{25.RDS}{\longrightarrow} 2HCHOX + XO$
26	$HCHOX + XO \overset{fast}{\longrightarrow} CO + H_2O + 2X$
27	$CH_3COOH.XO + XO \overset{27.RDS}{\longrightarrow} 2HCHOXO$
28	$HCHOXO + XO \overset{fast}{\longrightarrow} CO_2 + H_2O + 2X$
29	$CO + XO \overset{29.RDS}{\longrightarrow} CO_2 + X$
30	$COXOH + XOH \overset{30.RDS}{\longrightarrow} CO_2 + H_2O + 2X$

Linke et al. [10] also consider that two catalytic centers are required to explain the reaction pathways: oxidation of ethane to ethylene, formation of acetic acid from ethane via a surface intermediate and total oxidation is ascribed to one catalytic center. The second center exclusively catalyzes the oxidation of ethylene to acetic acid via the Wacker mechanism which is related to hydroxyl groups forming the active center. Hence, they proposed that formation of acetic acid from ethylene can be accelerated to a certain degree with increase in water to the feed. For the consumption of ethane, Thorsteinson [1] speculates that two sites are involved in the ethane partial oxidation reaction and suggests that the primary product of oxydehydrogenation of ethane is ethylene only and that acetic acid and carbon oxides are formed by the subsequent oxidation of ethylene. The present study suggests that the adsorbed ethylene species on the XO center reacts in parallel routes based on Eley-Rideal mechanism [steps 15, 17, 19 and 22] to produce CH_3COOH and CO_2 consistent with the selectivity behavior shown in Fig. 5.

Acetic acid is formed by reaction of an oxygen center (XO) with intermediate species of ethylene (step 16). An alternate route for the production of acetic acid is the reaction of ethylene species with the (XOH) oxygen center forming hydroxylated species as in step 17. This step is considered as a rate determining step. The hydroxylated species subsequently reacts with the XO center to form acetic acid (steps 18a, 18b, 18c). This route accounts for significant increase in acetic acid production with addition of water in the feed. Parallel reactions of the ethylene C_2H_4XO species produce CO_x (step 19 and 22). Acetic acid can further oxidize to CO and CO_2 (steps 25–30).

Analysis of the ERR model showed that ethane reaction through the ZOH route (Fig. 9) is not significant and no change in ethane conversion was observed with variation in water in the feed. So,

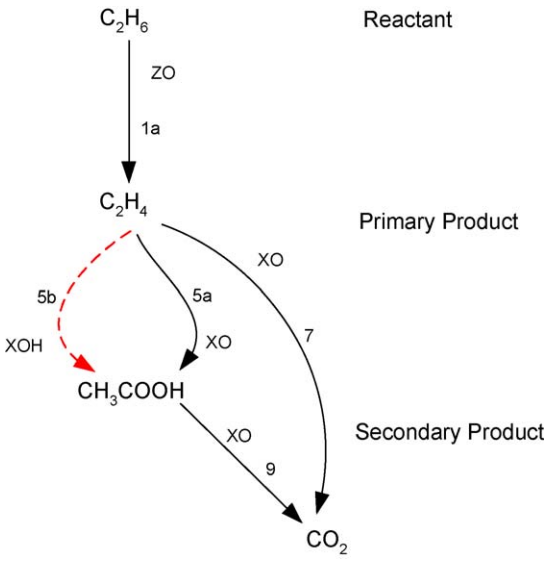

Fig. 10. Modified reaction scheme based on non-steam differential reactor data.

reaction through route 1b has been excluded from the model expressions for the ethane oxidation. The reactions ethylene to CO and acetic acid to CO were also found to be insignificant at the low conversions and at lower temperatures and hence reactions through routes 6, 8 and 10a and 10b have been removed from the network. The modified reaction scheme is shown in Fig. 10 and the corresponding modified ERR Model rate equations are presented in Table 3.

3.5. Estimation of model parameters

The equations of ERR (Eley-Rideal-Redox) model after excluding rate expressions for insignificant reactions are presented in Table 3. The models were evaluated by using MATLAB (ODE 45 and LSQCURVEFIT) least square fitting of the kinetic parameters. The evaluation of reaction rate parameters was conducted using experimental data at different reaction temperatures. In order to take into account the temperature dependence of the experimental data, the specific rate constants were expressed as Arrhenius type of temperature-dependent functions. The optimization criteria are that all the rate and equilibrium constants had to be positive, the activation energies for reaction positive, and the heat of adsorption ($-\Delta H$) positive, all consistent with physical principles. The optimization criteria used was based on a minimum sum of squares criteria defined by

$$\mathrm{SSQ} = \sqrt{\sum_{i=1}^{N}(c_{i,\mathrm{exp}} - c_{i,th})^2}$$

The model discrimination was carried out based on correlation coefficients (R^2), lowest sum of square (SSQ) residuals, smallest individual parameter confidence intervals. The adequacy of each model parameters was further established by analyzing their physical significance and through statistical analysis such as smallest confidence intervals and minimum values of the cross-correlation coefficients. Estimated parameters with confidence limits based on ERR Model for reaction scheme in Fig. 10 are given in Table 4.

The Arrhenius/van't Hoff plots for the model parameters are shown in Fig. 11a and b, respectively, and it can be observed that the figures follow the expected Arrhenius and van't Hoff relationships. The mean deviation between the experimental and

Table 4
Estimated parameters based on ERR Model.

Parameters	E or ΔH (kJ/mol)	A	95% confidence for E or ΔH
k_{1a}	108.2	1.46E+09	±2.75
k_b	91.20	1.19E+09	±6.92
k_{5a}	138.6	3.68E+13	±204
k_{5b}	116.0	2.51E+11	High
k_7	190.3	8.84E+17	±122
k_9	141.9	4.45E+13	±262
K_3	−56.80	1.39E−06	±66.3
K_4	−43.17	2.09E−05	±40.5
K_{12}	−96.56	2.49E−10	High
K_{13}	−114.5	5.57E−12	High
K_{14}	−124.0	4.62E−13	High
A_1	99.37	2.61E+09	±46.4
A_2	70.42	2.82E+06	High
K_{24}	−35.44	2.98E−04	High

Table 3
ERR Model rate equations for reaction network in Fig. 10.

At site Z: *Ethane to ethylene*

$$r_{1a} = \frac{k_b k_{1a} C_{C_2H_6} (A_1 C_{O_2})^{1/2}}{\left\{\nu_1 k_{1a} C_{C_2H_6}\left[1 + (A_1 C_{O_2})^{1/2} + (K_3 C_{H_2O})^{1/2}(A_1 C_{O_2})^{1/4}(1 + K_4 C_{H_2O})\right] + k_b (A_1 C_{O_2})^{1/2}\right\}}$$

where $A_1 = (K_1 K_2)$

At site X: *Ethylene oxidation*

$$r_{5a} = \frac{k_{5a} K_{13} C_{C_2H_4} (A_2 C_{O_2})^{1/2}}{1 + (A_2 C_{O_2})^{1/2}\left[1 + K_{13} C_{C_2H_4} + K_{24} C_{CH_3COOH} + \sqrt{K_{12} C_{H_2O}}(A_2 C_{O_2})^{-1/4}(1 + K_{14} C_{H_2O})\right]}$$

$$r_{5b} = \frac{k_{5b} K_{13} C_{C_2H_4} (K_{12} C_{H_2O})^{1/2} (A_2 C_{O_2})^{1/2}}{1 + (A_2 C_{O_2})^{1/2}\left[1 + K_{13} C_{C_2H_4} + K_{24} C_{CH_3COOH} + \sqrt{K_{12} C_{H_2O}}(A_2 C_{O_2})^{-1/4}(1 + K_{14} C_{H_2O})\right]}$$

$r_5 = r_{5a} + r_{5b}$, where $A_2 = (K_{10} K_{11})$

$$r_7 = \frac{k_7 K_{13} C_{C_2H_4} (A_2 C_{O_2})}{\left\{1 + (A_2 C_{O_2})^{1/2}\left[1 + K_{13} C_{C_2H_4} + K_{24} C_{CH_3COOH} + \sqrt{K_{12} C_{H_2O}}(A_2 C_{O_2})^{-1/4}(1 + K_{14} C_{H_2O})\right]\right\}^2}$$

$$r_9 = \frac{k_9 K_{24} C_{CH_3COOH} (A_2 C_{O_2})}{\left\{1 + (A_2 C_{O_2})^{1/2}\left[1 + K_{13} C_{C_2H_4} + K_{24} C_{CH_3COOH} + \sqrt{K_{12} C_{H_2O}}(A_2 C_{O_2})^{-1/4}(1 + K_{14} C_{H_2O})\right]\right\}^2}$$

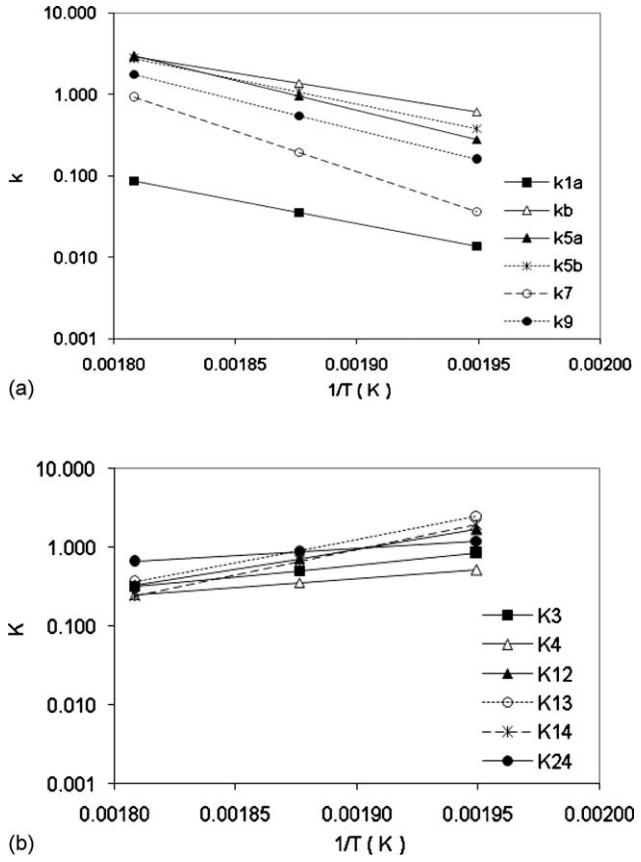

Fig. 11. (a) Arrhenius plot—rate constants versus $1/T$ based on non-steam data. (b) van't Hoff plot—equilibrium constants versus $1/T$ based on non-steam data.

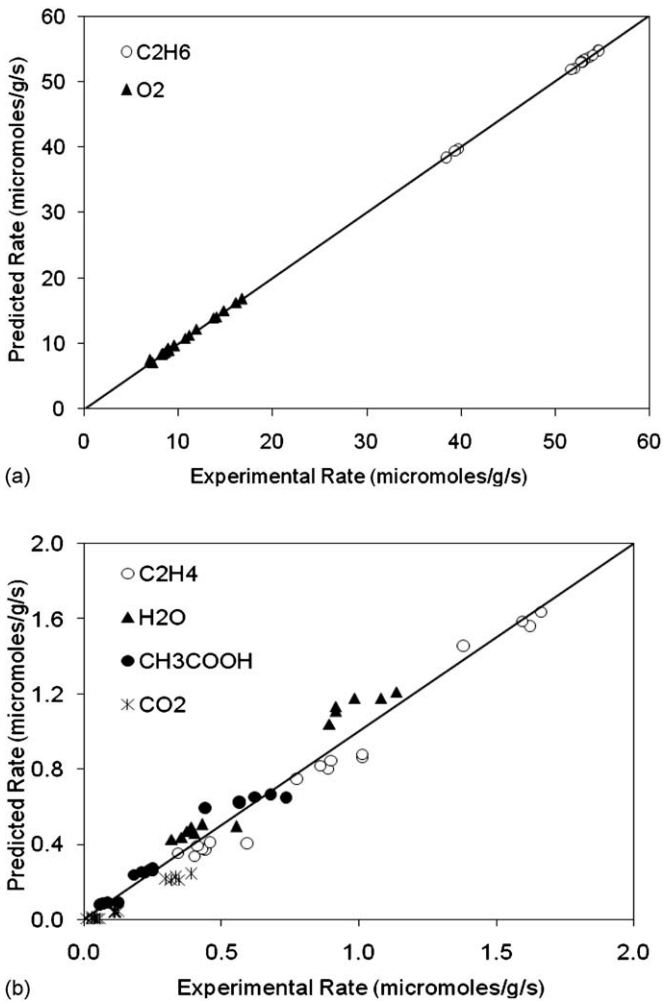

Fig. 12. (a) Parity plot of reactants consumption rates using ERR Model. (b) Parity plot of products formation rates using ERR Model.

predicted reaction rates obtained is 17.2%. High deviations are observed in prediction of CO_2 data and this may be attributed to error in the analysis of small quantities of CO_2 in the product stream. If the mean deviation is calculated excluding the error involved due to CO_2, the mean deviation reduces from 17.2% to 8.5%.

The parity plots for the rates of reactants and products are illustrated in Fig. 12a and b, respectively. The predicted reactants rates fit the experimental data in an excellent manner with even distribution of error along the x-axis within a narrow range of ±5%. The fit is reasonable in case of products rates with distribution of error along the x-axis within a range of ±30%. Some deviations are observed in predicted water and CO_2 reaction rates.

The order of magnitude of the activation energies estimated based on the ERR Model is similar to that of values reported in the literature [1,4,9]. The frequency factors for all the rate constants vary from 10^9 to 10^{17} typically in units of micromole/g cat/s. For first order homogeneous reactions the value should typically are around 10^{15} s^{-1} or less [18]. Thus the order of magnitude of the frequency factors appears reasonable.

4. Conclusion

The kinetics and mechanism of C_2H_6 oxidation to C_2H_4 and CH_3COOH over MoV type catalyst has been studied. The primary product of C_2H_6 oxidation is C_2H_4 which through consecutive reactions transforms to acetic acid and to products of deep oxidation such as CO_x. The reaction rate in both directions proportionally increases with the increase of partial pressure of C_2H_6, which shows that the reaction order for C_2H_6 in both directions is close to 1. The effect of oxygen concentration to the rate of ethylene and acetic acid formation reactions is not significant which shows that the surface of the catalyst at investigated conditions is close to fully oxidized. Experimentally observed significant positive effect of water to acetic acid selectivity has been explained on the basis of surface OH^- groups leading to the additional parallel route of CH_3COOH formation. Eley-Rideal-Redox kinetic model based on two-site reaction mechanism has been evaluated for description of experimental results on C_2H_6, O_2 effect and chemical contribution of water to the reaction pathways. The ERR model represents data adequately with an overall average deviation of about 8.5%.

Chemical contribution of water to the reaction mechanism through formation of surface OH^- groups show the existence of acid base interaction of intermediate ethylene with surface. This principal allows improving acetic acid formation selectivity through modification of acidic properties of the catalyst. The chemical contribution of water to kinetic behavior of the reaction on MoV type catalyst through formation of surface hydroxyl groups has been proved by isotopic experiments, which is the subject of a later publication.

Acknowledgments

We would like to express our appreciations to SABIC for their financial support under project # CRP2205. We also acknowledge the support from Center of Research Excellence in Petroleum

Refining and Petrochemicals at King Fahd University of Petroleum & Minerals (KFUPM) established by the Ministry of Higher Education, Saudi Arabia. Special thanks are due to King Fahd University of Petroleum and Minerals, Dhahran, Saudi Arabia.

References

[1] E.M. Thorsteinson, F.G. Young, P.H. Kasai, J. Catal. 52 (1978) 116–132.
[2] R. Burch, R. Swarnakar, Appl. Catal. 70 (1991) 129–148.
[3] O. Desponds, R.L. Keisiki, G.A. Somorjai, Catal. Lett. 19 (1993) 17–32.
[4] A.A. Saberi-Moghaddam, A. Adesina, D.L. Trimm, Sci. Technol. Catal. 92 (1994) 197–202.
[5] K. Ruth, R. Burch, R. Kieffer, J. Catal. 175 (1998) 27–39.
[6] W. Ueda, N.F. Chen, K. Oshihara, Kinet. Catal. 40 (1999) 401–404.
[7] N.F. Chen, W. Ueda, K. Oshihara, Chem. Commun. 6 (1999) 517–518.
[8] A.H. Fakeeha, Y.M. Fahmy, M.A. Soliman, S.M. Alwahabi, J. Chem. Technol. Biotechnol. 75 (2000) 1160–1168.
[9] D. Linke, D. Wolf, M. Baerns, O. Timpe, R. Schloegl, S. Zeyss, U. Dingerdissen, J. Catal. 205 (2002) 16–31.
[10] D. Linke, D. Wolf, M. Baerns, S. Zeyss, U. Dingerdissen, J. Catal. 205 (2002) 32–43.
[11] D. Linke, D. Wolf, M. Baerns, S. Zeyss, U. Dingerdissen, L. Mleczko, Chem. Eng. Sci. 57 (2002) 39–51.
[12] M. Rouessel, M. Bouchard, E. Bordes-Richard, K. Karim, S. Al-Sayari, Catal. Today 99 (2005) 77–87.
[13] R. Grabowski, J. Sloczynski, Chem. Eng. Process. 44 (2005) 1082–1093.
[14] K. Karim, A. Mamedov, M.H. Al-Hazmi, N. Al-Andis, Reac. Kinet. Catal. Lett. 80 (2005) 3–11.
[15] J.M. Galownia, A.P. Wight, A. Blanc, J.A. Labinger, M.E. Davis, J. Catal. 236 (2005) 356–365.
[16] Q. Smejkal, D. Linke, M. Baerns, Chem. Eng. Process. 44 (2004) 421–428.
[17] Y.A. Ahmed, Steady state and periodic operation studies of the partial oxidation of propylene, Ph.D. Dissertation, University of Waterloo, 1990.
[18] B.W. Wojciechowski, N.M. Rice, Experimental Methods in Kinetic Studies, Revised ed., Elsevier Science B.V., Amsterdam, 2003.
[19] D.E. Mears, Ind. Eng. Chem. Proc. Des. Dev. 10 (1971) 541.
[20] M.D. Argyle, K. Chen, A.T. Bell, E. Iglesia, J. Phys. Chem. B 106 (2002) 5421–5427.
[21] K. Karim, S. Kareemuddin, US Patent 6028221, 2000.
[22] S. Jitkarnka, Oxidation dehydrogenation of ethane to ethylene and acetic acid by multicomponent mixed oxide catalysts, Ph.D. Dissertation, Texas A&M University, 2001.
[23] L. Tessier, E. Bordes, M. Gubelmann-Bonneau, Catal. Today 24 (1995) 335–340.
[24] G.I. Panov, K.A. Dubkov, E.V. Starokon, Catal. Today 117 (2006) 148–155.
[25] R. Sehgal, Ethane oxidative dehydrogenation at low temperatures, M.S. Thesis, Chemical Engineering, Dalhousie University, 2007.
[26] L. Capek, J. Adam, T. Grygar, R. Bulanek, L. Vradman, G. Kosova-Kucerova, P. Cicmanec, P. Knotek, Appl. Catal. A 342 (2008) 99–106.